CILAMCE 2017
Florianópolis - Santa Catarina - Brazil

# NUMERICAL INVESTIGATION OF TURBULENT NATURAL CONVECTION IN ENCLOSED CAVITIES

**Rebeca Pereira Marcondes**

**Francisco Marcondes**

rebecapereiramarc@hotmail.com

marcondes@ufc.br

Federal University of Ceará

Technology Center, Department of Metallurgical Engineering and Material Science, 60440-554, Ceara, Fortaleza, Brasil

***Abstract.*** *Natural convection in enclosed cavities is widely investigated phenomenon because it has a large spectrum of application in engineering, which include cooling of fluids, ventilation of buildings, food processing and storing, solar collectors, among them. This subject has been investigated through analytical, numerical, and experimental procedures. However, some important issues related to this problem still need to be understood, especially for turbulent flows. In this work, turbulent fluid flow, for two and three-dimensional enclosed cavities with several aspect ratio, using oil as a work fluid, is investigated. The numerical analysis is performed using the ANSYS CFX© software in conjunction with the k-$\omega$ and SST models. All simulations are performed for two and three-dimensional cavities, with isothermal vertical walls and horizontal adiabatic walls for a wide Rayleigh numbers ($3.7 \times 10^8 \leq Ra \leq 10^{11}$) using an Element based Finite Volume Method (EbFVM) in conjunction with unstructured grids. The results are presented in terms of isotherms, streamlines, temperature profiles and average Nusselt number.*

***Keywords:*** *Natural Convection, EbFVM, Turbulence flow, k-$\omega$ model, SST model*

# 1 INTRODUCTION

Natural convection is a phenomenon present in various engineering applications such as cooling of electric components, cooling of nuclear reactors, solar collectors and combustion processes. This problem has been investigated through numerical, analytical and experimental procedures by numerous researchers. However, there are still many problems to be understood, especially for turbulent regime. The focus of this work is in the turbulent flows, since not all available models pay respect to the actual physical models of turbulence, therefore it requires more caution in choosing the turbulence model to model a certain problem.

The Wilcox (1986), k-$\omega$, model is a promising approach for the analysis of internal flows with large Rayleigh number, since there are several studies in the literature showing the k-$\omega$ model in a good agreement with experimental results such as Rocha et al. (2015) who examined a wide range of Rayleigh numbers for air as a work fluid, including turbulent cases that were experimentally investigated by Ampofo and Karayiannis (2003) and Sharif and Liu (2003). A comparison between the numerical and experimental local Nusselt was made and the results were in a good agreement. Marcondes and Marcondes (2016) also obtained good numerical outcome with the experimental investigation by Lankhorst (1991) with a correlation between the $\overline{Nu}$ and the $Ra$ number for water as a work fluid for $10^6 \leq Ra \leq 10^8$ and for $Ra = 3 \times 10^{10}$ for air.

Other recent investigations were made for different parameters for a finer understanding of the effects on the fluid pattern for a incompressible fluid with a thermal activity inside the cavity (Purusothaman et al., 2015), for various cavities geometry such as trapezoidal cavities (Silva et al., 2012), cubic cavities (Pallares et al., 2002) and aspect ratio (Trias (2007), Ganguli et al., 2009).

This work addresses the numerical investigation of the turbulent natural convection for several Rayleigh numbers and several aspect ratios of the cavity using ($Pr = 464$) as working fluid, where the walls in the y-axis are differently heated and the remains walls are adiabatic.

For most of the investigations, we have employed the k-$\omega$ model, but for validation purposes the BSL (Baseline) and the SST (Shear Stress Transport) were also used, both models are combinations of k-$\omega$ and k-$\varepsilon$ model. The results are shown in terms of isotherms, streamlines, velocity and temperature profiles and average Nusselt numbers.

# 2 MATHEMATICAL FORMULATION

The employed considerations were: all the fluid properties were constant, except for the buoyancy term along the y-axis in the Navier-Strokes equations, steady state (the transient term is present in the equations to capture the oscillations from the turbulent flow), incompressible fluid flow and thermal radiation effects were omitted.

$$\frac{\partial \rho}{\partial t} + \frac{\partial}{\partial x_j}(\rho U_j) = 0 \tag{1}$$

$$\frac{\partial \rho U_i}{\partial t} + \frac{\partial}{\partial x_j}(\rho U_i U_j) = -\frac{\partial p'}{\partial x_i} + \frac{\partial}{\partial x_j}\left[\mu_{eff}\left(\frac{\partial U_i}{\partial x_j} + \frac{\partial U_j}{\partial x_i}\right)\right] + S_M \tag{2}$$

$$\frac{\partial T}{\partial t} + \frac{\partial U_j T}{\partial x_j} = \frac{\partial}{\partial x_j}\left[\left(\frac{\nu}{Pr} + \frac{\nu_t}{\sigma_t}\right)\frac{\partial T}{\partial x_j}\right] \tag{3}$$

Moreover, the turbulent problems were solved with the k-$\omega$ equations, which assumes that the turbulent viscosity $\mu_t$ is related to the turbulent kinetic energy $k$ and the turbulent frequency $\omega$.

$$\frac{\partial \rho k}{\partial t} + \frac{\partial}{\partial x_j}(\rho U_j k) = \frac{\partial}{\partial x_j}\left[\left(\mu + \frac{\mu_t}{\sigma_k}\right)\frac{\partial k}{\partial x_j}\right] + P_k - \beta' \rho k \omega \tag{4}$$

$$\frac{\partial \rho \omega}{\partial t} + \frac{\partial}{\partial x_j}(\rho U_j \omega) = \frac{\partial}{\partial x_j}\left[\left(\mu + \frac{\mu_t}{\sigma_\omega}\right)\frac{\partial \omega}{\partial x_j}\right] + \alpha \frac{\omega}{k} P_k - \beta \rho \omega^2 \tag{5}$$

$$P_k = \mu_t \left(\frac{\partial U_i}{\partial x_j} + \frac{\partial U_j}{\partial x_i}\right)\frac{\partial U_i}{\partial x_j} - \frac{2}{3}\frac{\partial U_k}{\partial x_k}\left(3\mu_t \frac{\partial U_k}{\partial x_k} + \rho k\right) \tag{6}$$

$$\mu_t = \rho \frac{k}{\omega} \tag{7}$$

The constants of the k-$\omega$ model are:

$$\beta' = 0.09 \tag{8}$$
$$\alpha = 5/9 \tag{9}$$
$$\beta = 0.075 \tag{10}$$
$$\sigma_k = 2 \tag{11}$$
$$\sigma_\omega = 2 \tag{12}$$
$$\tag{13}$$

Since the further models used are blended between the k-$\omega$ and the k-$\varepsilon$ model, differing by only one constant and the expression for turbulent eddy viscosity. The k-$\varepsilon$ model is also presented, which assumes that k is the turbulent kinetic energy and $\varepsilon$ is the turbulent dissipation.

$$\frac{\partial}{\partial t}(\rho k) + \frac{\partial}{\partial x_j}(\rho U_j k) = \frac{\partial}{\partial x_j}\left[\left(\mu + \frac{\mu_t}{\sigma_k}\right)\frac{\partial k}{\partial x_j}\right] + P_k - \rho \varepsilon \tag{14}$$

$$\frac{\partial}{\partial t}(\rho \varepsilon) + \frac{\partial}{\partial x_j}(\rho U_j \varepsilon) = \frac{\partial}{\partial x_j}\left[\left(\mu + \frac{\mu_t}{\sigma_\varepsilon}\right)\frac{\partial \varepsilon}{\partial x_j}\right] + \frac{\varepsilon}{k}(C_{\varepsilon 1} P_k - C_{\varepsilon 2} \rho \varepsilon) \tag{15}$$

The is the turbulence production due to viscous forces, is the same used in k-$\omega$ model (Eq. 6) the difference is in the $\mu_t$, given by:

$$\mu_t = C_\mu \rho \frac{k^2}{\varepsilon} \tag{16}$$

The constants of the k-$\varepsilon$ model are:

$$C_{\varepsilon 1} = 1.44 \tag{17}$$
$$C_{\varepsilon 2} = 1.92 \tag{18}$$
$$\sigma_k = 1 \tag{19}$$
$$\sigma_\varepsilon = 1.3 \tag{20}$$
$$\tag{21}$$

In the above equations, $U_i$ (m/s) is the velocity along each axis , $\rho$ (kg/m$^3$) is the fluid density, T (K) is the fluid temperature, $p'$ (Pa) is the modified pressure , $P_k$ (kg/ms$^3$) is the turbulence production rate , $\sigma_t$ is the turbulent Prandtl number (Pr = 464), $\nu$ (m$^2$/s) is the kinematic viscosity , $\nu_t$ (m$^2$/s) is the kinematic turbulent viscosity, $\mu$ (kg/ms) is the dynamic viscosity, k ($\mathrm{m}^2/\mathrm{s}^2$) is the kinetic turbulent energy , $\omega$ ($\mathrm{m}^2/\mathrm{s}^2$) is the turbulent dissipation rate, t (kg/m s) is the turbulent viscosity and $\mu_{eff} = \mu + \mu_t$ (if the flow is laminar $\mu_t = 0$) . The momentum source $S_M$ along the y-axis is given by $S_M = -g(T - T_0)$, where $T_0$ (K) is the reference temperature, g (m/s$^2$) is the gravitational acceleration and $\beta$ (1/K) is the thermal expansion coefficient of the fluid.

Although we are interested in the steady state regime, we kept the transient terms in the conservation equations because, it is a way to treat the coupling between the equations and the nonlinearities in order to reach the steady regime.

## 2.1 Boundary conditions

The boundary conditions for a three dimensional cavity are found above, the same boundary conditions are used for the two dimensional modeling except by the z-axis which is neglected.

$$T(x=0,y,z) = T_c \qquad u(x=0,y,z) = \mathrm{v}(x=0,y,z) = 0 = w(x=0,y,z) = 0 \tag{22}$$

$$T(x=L,y,z) = T_h \qquad u(x=L,y,z) = \mathrm{v}(x=L,y,z) = 0 = w(x=L,y,z) = 0 \tag{23}$$

$$\left.\frac{\partial T}{\partial y}\right)_{y=0} = 0 \qquad u(x,y=0,z) = \mathrm{v}(x,y=0,z) = 0 = w(x,y=0,z) = 0 \tag{24}$$

$$\left.\frac{\partial T}{\partial y}\right)_{y=H} = 0 \qquad u(x,y=H,z) = \mathrm{v}(x,y=H,z) = 0 = w(x,y=H,z) = 0 \tag{25}$$

$$\left.\frac{\partial T}{\partial z}\right)_{z=0} = 0 \qquad u(x,y,z=0) = \mathrm{v}(x,y,z=0) = 0 = w(x,y,z=0) = 0 \tag{26}$$

$$\left.\frac{\partial T}{\partial z}\right)_{z=W} = 0 \qquad u(x,y,z=W) = \mathrm{v}(x,y,z=W) = 0 = w(x,y,z=W) = 0 \tag{27}$$

The boundary conditions used to solve the equations for k and $\omega$ are provided by the automatic near wall treatment, which automatically turn from wall functions to a low-Reynolds near wall formulation as the mesh is refined.

The dimensionless numbers used as parameters were the Rayleigh ($Ra$), Prandtl ($Pr$ = 464), average and local Nusselt (respectively, $\overline{Nu}$ and $Nu$) numbers. The dimensionless groups investigated in this work are given by:

$$Ra = \frac{g\beta(T_h - T_c)x^3}{\nu\alpha} \tag{28}$$

$$Pr = \frac{\nu}{\alpha} \tag{29}$$

$$Nu = \frac{hy}{k} \tag{30}$$

$$\overline{Nu} = \frac{1}{H}\int_0^H Nu dy \tag{31}$$

Where $y$ (m) is the local distance along the height of the cavity (H), $\alpha$ (m$^2$/s) is the thermal diffusivity, $h$ (W/m$^2$K) is the convective heat transfer coefficient of the flow and, $k$ (W/m K) is the thermal conductivity of the fluid.

## 3 CAVITY CONFIGURATION

Figure 1 presents geometries of the flow domain and examples of meshes used in the work. In Fig. 1a the cavity with ratio aspect (A = H/L) is equal to 1, but, in this investigation, for two-dimensional cavities, the aspect ratio equal to 5 was used as well. The ratio aspect for three-dimensional case studies was kept equal to 5.

As shown in Fig. 1(a) and Fig. 1(c), vertical left and right walls of the square cavity are heated and cooled, respectively, at constant temperatures $T_h$ and $T_c$, where $T_h > T_c$, while the remain walls of the cavity were kept adiabatic.

The refinement was focused on the cavities close to the boundaries where the gradients due to its temperature differences are expected to be higher as presented in Fig. 1(b) and Fig. 1(d).

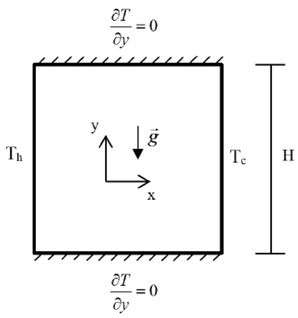


**(a) Cavity configuration for two-dimensional with A = 1**

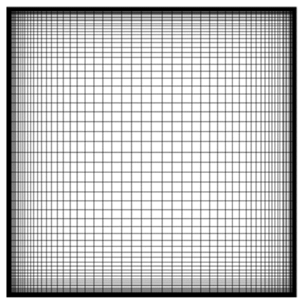

**(b) Mesh with grid refinement 140 × 140 for two-dimensional with A = 1**

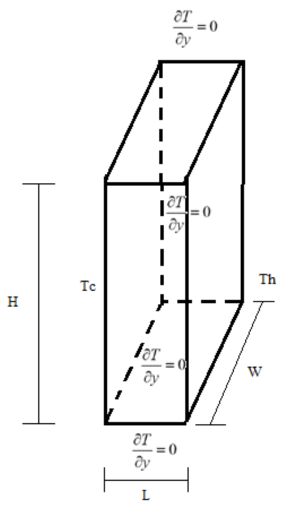


**(c) Cavity configuration for three-dimensional with A = 5**

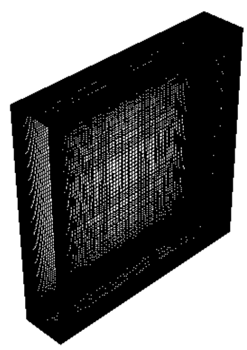

**(d) Mesh with grid refinement 60 × 120 × 120 for three-dimensional with A = 5**

**Figure 1: Cavities and grid configurations**

# 4 RESULTS AND DISCUSSION

The results and discussion section is divided into two parts and shows the results in terms of isotherms, velocity and temperature profiles and the average Nusselt number ($\overline{Nu}$). The first part presents the mesh refinement study and the comparison between k-$\omega$, SST, and BSL turbulence models. In the second part, there the temperature profiles comparison between 2D and 3D cases and the results in terms of streamlines, isotherms, $\overline{Nu}$, velocity and temperature profiles, using oil as a work fluid (Pr = 464), ranging from $Ra = 10^9$ to $10^{11}$ and for $Ra = 3.7 \times 10^8$. The error for mass, momentum and energy for was considered less than $10^{-7}$.

## 4.1 Mesh refinement study

Table 1 presents the mesh refinement study that was performed for the 3D simulations and the results were considered mesh independent when the $\overline{Nu}$ number presented an error less then $0.3\%$. We chose the $60 \times 120 \times 120$ non-uniform grid for all the three-dimensional simulations and $60 \times 100$ for two-dimensional.

In Tab. 2 for the propose of comparision between turbulence model for $Ra = 3.7 \times 10^8$, simulations were made for BSL and SST models also, as the table shown, the error in relation to the k-$\omega$ model is less then 0.1 $\%$ for the BSL model and less then 0.3$\%$ for the SST, meaning those models have a similar approach for this case.

**Table 1: $\overline{Nu}$ for different grids in 3D** $Ra = 3.7 \times 10^8$

| Mesh | k-$\omega$ |
|---|---|
| $20 \times 50 \times 50$ | 49.7436 |
| $40 \times 90 \times 90$ | 45.732 |
| $50 \times 100 \times 100$ | 44.6477 |
| $60 \times 120 \times 120$ | 44.9981 |
| $100 \times 100 \times 100$ | 44.9009 |
| Error ($\%$) | 0.2167 |

**Table 2: $\overline{Nu}$ for different turbulence models in 2D** $Ra = 3.7 \times 10^8$

| Mesh | k-$\omega$ | SST | BSL |
|---|---|---|---|
| $60 \times 100$ | 44.8322 | 44.6475 | 44.8131 |
| Error ($\%$) | - | 0.369 | 0.042 |

## 4.2 Temperature and velocity profiles, isotherms and streamlines

Figure 2, presents the temperature profiles for the 2D and 3D cavities, at three different elevations for oil as a work fluid and $Ra = 3.7 \times 10^8$ for the aspect of the cavity equal to 5. As we can notice, the temperature profiles are very close to one another, especially in the region close to the walls. Therefore, since the 3D simulations are much more expensive, particularly for refined meshes, we decided to run all the remaining cases using 2D cavities.

Numerical simulations were performed for $Pr = 464$, for $10^9 \leq Ra \leq 10^{10}$ for two-dimensional cavity with $A = 1$ and for $Ra = 3.7 \times 10^8$ two and three-dimensional cavities with $A = 5$. The fluid motion and heating patterns are studied along the vertical heated and cooled walls of the cavities and adiabatic on the remains axis surfaces.

Figures 3 and 4 present the isotherms and streamlines for in the range of $10^9 \leq Ra \leq 10^{10}$ for 2D cavities. As shown, when the $Ra$ is increased, the normal wall temperature gradient increases, and the convection becomes more dominant. It is also observed that the center of the cavity becomes more stratified as it can be observed by the isotherms patterns illustrated in Figs. 3(a) through 3(c).

Figure 5 shows the velocity profile inside the 2D cavity for $Ra = 3.7 \times 10^8$ and A = 5. The velocity close to the walls, where the temperature gradient is higher than in the center of the cavity, where the velocity is almost zero. Also, the velocity vectors are indicating the fluid flow direction close to left wall is in upward, and in the right wall is in downward direction. From this figure, we can observe that the fluid motion is mainly located close the vertical walls and is stagnated in the center of the cavity

Figure 6 shows the streamline for a 3D cavity with A = 5 $Ra = 3.7 \times 10^8$. Once again, we can observe from that figure that the largest velocity are close to the wall and the fluid around the center of the cavity is almost stagnant.

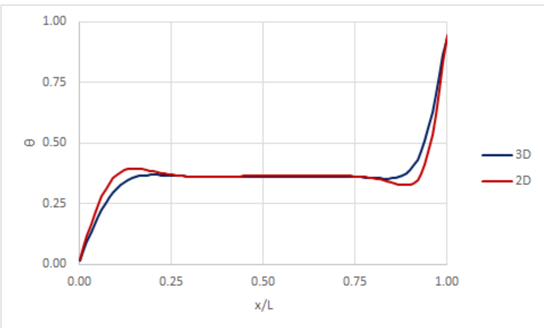


**(a) y/H = 0.25**

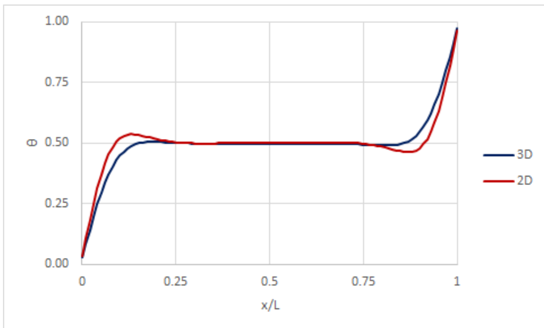


**(b) y/H = 0.5**

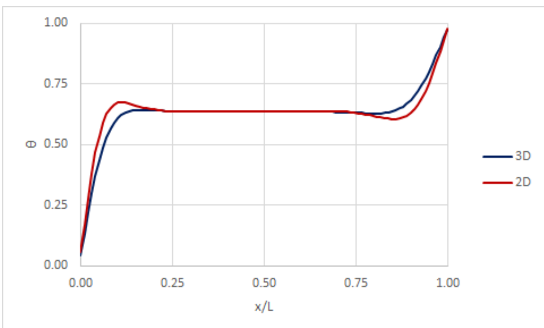


**(c) y/H = 0.75**

**Figure 2: Temperature profile for three and two dimensional cavities for A =5**

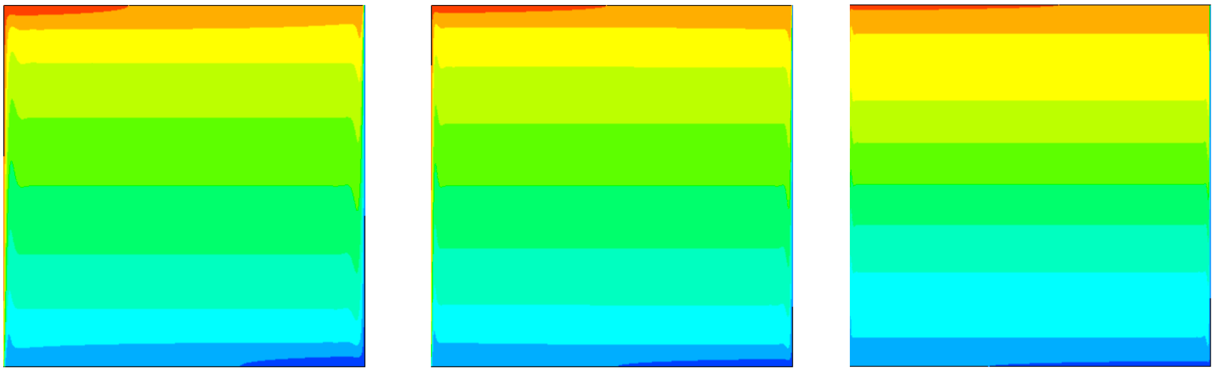

**(a)** $Ra = 10^9$ **(b)** $Ra = 10^{10}$ **(c)** $Ra = 10^{11}$

**Figure 3: Isotherms for A =1**

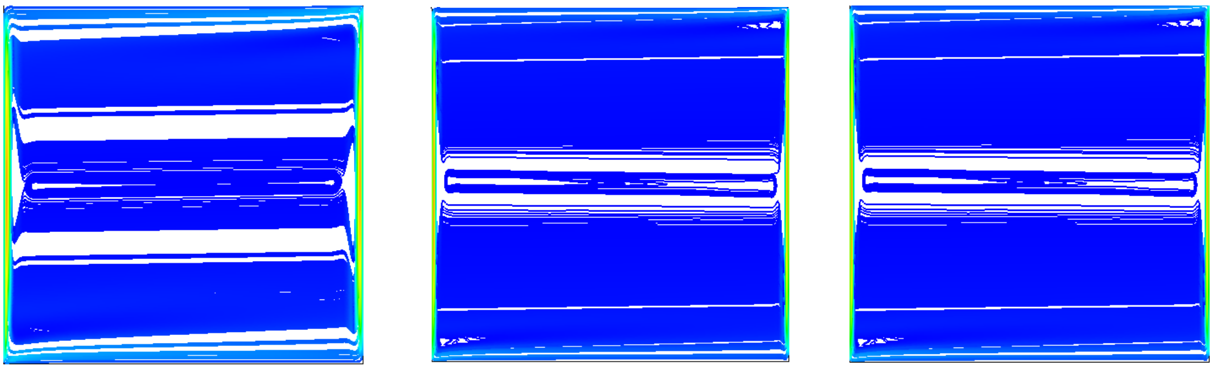

**(a)** $Ra = 10^9$ **(b)** $Ra = 10^{10}$ **(c)** $Ra = 10^{11}$

**Figure 4: Streamlines for A =1**

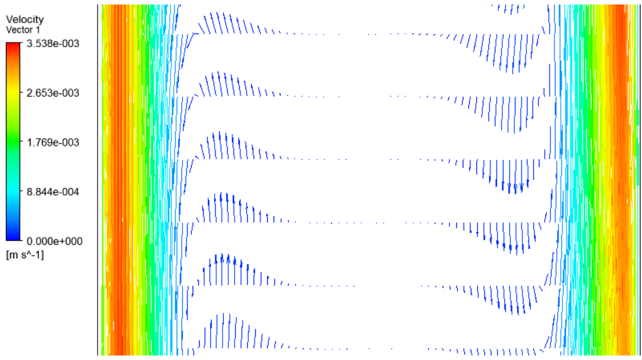


**Figure 5: Velocity profile for two dimensional with $Ra = 3.7 \times 10^8$ (A = 5)**

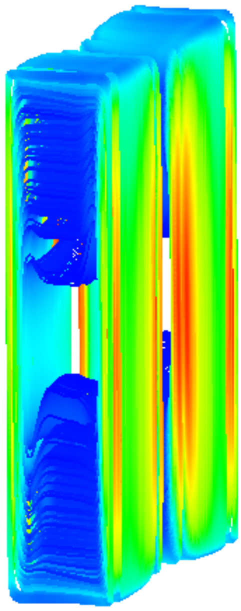

**Figure 6: Streamline for three dimensional with $Ra = 3.7 \times 10^8$ (A = 5)**

# 5 CONCLUSIONS

The present work investigated the turbulent natural convection in 2D and 3D enclosed cavities with two different aspects ratio (A = 1 and A =5), for Prandtl number equal to 464, and a range of Rayleigh numbers ($3.7 \times 10^8 \leq Ra \leq 10^{10}$). Most of the results were obtained with the k-$\omega$ model, but the SST and BSL models were also used. The governing equations were solved through the EbFVM (Element based Finite-Volume Method), using the commercial simulator ANSYS CFX©. The results were presented in terms of isotherms, streamlines, average Nusselt numbers and velocity and temperature profiles.

For each $Ra$ investigated a mesh refinement was performed, using the average Nu as a parameter. The solution was satisfactory when the variation was lower than $0.3\%$.

Most of the simulations were made with a 2D results were close to the 3D results, especially the gradient of temperature close to the isothermal walls. Also, it was noticed that the k-$\omega$, SST and BSL turbulence models had very similar results for the case where $Ra = 3.7 \times 10^8$ for 2D cavity; when we compared the avarege Nusselt obtained with the k-$\omega$ model with the one obtained with the SST model the diference was less $1\%$, and the difference between the k-$\omega$ and BSL was even smaller.

## REFERENCES

Cheesewright, R.; King, K.J.; Ziai, S., Experimental data for the validation of computer codes for the prediction of two-dimensional buoyant cavity flows, *ASME Winter Annual Meeting*, p. 75, 1986.

Lankhorst, A. M., Laminar and turbulent natural convection in cavities-numerical modelling and experimental validation, Ph.D. thesis, Technology University of Delft, The Netherlands, 1991.

Da Silva, A.; Fontana, E.; Mariani, V. C.; Marcondes, F., Numerical investigation of several physical and geometric parameters in the natural convection into trapezoidal cavities, *Int. J. Heat Mass Transfer*, v. 55, p. 6808-6818, 2012.

Marcondes, R. P.; Marcondes, F. . Investigation of laminar and turbulent natural convection in square cavities, *Congresso Brasileiro de Engenharia Quimica* (Cobeq), 2016, Fortaleza. .

Rocha, J. R. S. ; Marcondes, R. P. ; Lima, I. C. M. ; Marcondes, F. . Laminar and Turbulent Natural Convection in 2D-Square Cavities, *23rd ABCM International Congress of Mechanical Engineering* (COBEM), 2015, Rio de Janeiro.

Trias, F. X.; Soria, M.; Oliva, A.; Prez-Segarra, C. D., Direct numerical simulations of two and three-dimensional turbulent natural convection flows in a differentially heated cavity of aspect ratio 4, *Journal of Fluid Mechanics*, v. 586, p. 259-293, 2007.

Wilcox, D.C., Multiscale model for turbulent flows. *AIAA 24th Aerospace Sciences Meeting*, 1986.

Vieira, C. B., Computational simulation of natural convection in cavities holding a fluid with heat internal generation, M.Sc., (UFRRJ/COPPE, Nuclear energy program). Federal University of Rio de Janeiro, 2010. (In Portuguese).